Inorg. Chem. **1997,** *36,* 2826−2833

Multielectron Reduction of α-$[S_2Mo_{18}O_{62}]^{4-}$ in Aprotic and Protic Media: Voltammetric Studies

David M. Way,[†] **Alan M. Bond,***[,‡] **and Anthony G. Wedd***[,§]

Department of Chemistry, La Trobe University, Bundoora, Victoria 3083, Australia, Department of Chemistry, Monash University, Clayton, Victoria 3168, Australia, and School of Chemistry, University of Melbourne, Parkville, Victoria 3052, Australia

Received December 12, 1996[⊗]

Detailed voltammetric studies are reported of the reduction of α-$[S_2Mo_{18}O_{62}]^{4-}$ at glassy carbon and platinum macro- and microdisk electrodes (stationary and rotated) in acetonitrile and in 95/5 acetonitrile/water mixtures containing 0.02 M perchloric acid. Experiments at −30 °C and at short time scales in acetonitrile detect eight one-electron processes in the potential range 0.1 to −2.7 V versus Fc^+/Fc (Fc = ferrocene). The eight processes fall into four pairs. The differences in potential within each pair are remarkably constant (0.26 ± 0.02 V), as are the separations between adjacent pairs (0.60 ± 0.06 V). This periodicity is consistent with spin-paired $[Mo^{V}O]_2$-(μ-O) fragments providing a significant contribution to the overall superexchange stabilization. The influence of the following chemical reactions (primarily protonation by trace water) increases with the number of electrons added, although the five-electron reduced species $[S_2Mo_{18}O_{62}]^{9-}$ has a significant lifetime on the voltammetric time scale. In the presence of aqueous acid and at short time scales, eight chemically reversible processes are observed in the range 0 to −1.5 V in which two, two, two, two, four, four, two, and eight electrons, respectively, are transferred. The four pairs of one-electron processes found in acetonitrile occur as the first four overall two-electron reduction steps, separated by about 0.1, 0.2, and 0.3 V, respectively. Addition of a further 10 electrons occurs in a range of 0.3 V only and results in an 18-electron reduced species, stable on the voltammetric time scale. This corresponds to formal reduction of all Mo(VI) centers in α-$[S_2Mo_{18}O_{62}]^{4-}$ to Mo(V). The species is able to accept a further eight electrons in a series of unresolved processes.

Introduction[1]

Polyoxometalate cluster anions such as α-$[S_2Mo_{18}O_{62}]^{4-}$ (structure **I**) are reducible to mixed-valence compounds, commonly known as "poly blues" due to the presence of intervalence charge transfer transitions in the visible spectrum.[2−4] Multielectron reduction is observed for those anions which contain structural octahedra bearing a single terminal oxo ligand.[5−8] Reduction is accompanied by minor structural changes only, as the extra electrons enter orbitals that are essentially nonbonding. Thus, the reduced forms are class II mixed-valence compounds[9] in which thermally mobile electrons "hop" between octahedra.[2,3,10−23] As reduction proceeds, the anions acquire an increasing negative charge which encourages protonation. This lowers the negative charge, encouraging further reduction.

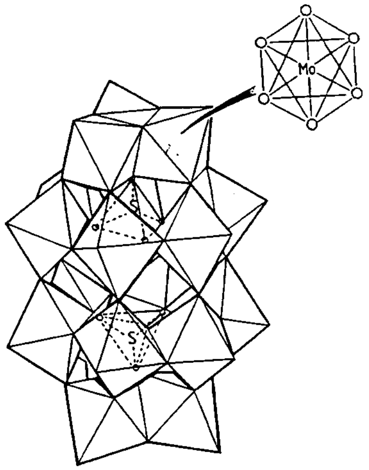

I

There are two inequivalent Mo sites in the idealized α-$[S_2Mo_{18}O_{64}]^{4-}$ anion (structure **I**: D_{3h} point symmetry).[24−27] Two

---

* Authors to whom correspondence should be addressed: a.bond@sci.monash.edu.au; t.wedd@chemistry.unimelb.edu.au.

[†] La Trobe University.

[‡] Monash University.

[§] University of Melbourne.

[⊗] Abstract published in *Advance ACS Abstracts,* May 15, 1997.

(1) Abbreviations: **I**−**VIII**, redox processes ocurring in MeCN solution; I−VIII, redox processes ocurring in 95/5 MeCN/H_2O (0.02 M $HClO_4$); Bu, *n*-butyl; *C*, concentration; *d*, diameter; *D*, diffusion coefficient; *E*, potential; E_{pa}, anodic peak potential; E_{pc}, cathodic peak potential; ΔE_p, difference between E_{pa} and E_{pc}; *F*, Faraday's constant; $E_{1/2}$, reversible half-wave potential; $\Delta E_{1/2}$, difference between two $E_{1/2}$ values; Fc, $Fe(\eta^5\text{-}C_5H_5)_2$; Hex, *n*-hexyl; *i*, current at potential *E*; i_L, limiting current; i_{pa}, current at E_{pa}; i_{pc}, current at E_{pc}; *n*, number of electrons transferred per mole; *T*, temperature; *v*, scan rate.

(2) Pope, M. T. *Heteropoly and Isopoly Oxometalates*; Springer-Verlag: Berlin, 1983; pp 101−117.

(3) Pope, M. T.; Müller, A. *Angew. Chem., Int. Ed. Engl.* **1991**, *30*, 34.

(4) *Polyoxometalates: From Platonic Solids to Anti-Retroviral Activity;* Pope, M. T., Müller, A., Eds.; Kluwer Academic Publishers: Dordrecht, The Netherlands, 1994.

(5) Papaconstantinou, E.; Pope, M. T. *Inorg. Chem.* **1967**, *6*, 1152.

(6) Pope, M. T.; Papaconstantinou, E. *Inorg. Chem.* **1967**, *6*, 1147

(7) Massart, R. *Ann. Chim.* **1969**, *4*, 285, 315, 441.

(8) Pope, M. T. *Inorg. Chem.* **1972**, *11*, 1973.

(9) Robin, M. B.; Day, P. *Adv. Inorg. Chem. Radiochem.* **1967**, *10*, 247.

(10) Prados, R. A.; Pope, M. T. *Inorg. Chem.* **1976**, *15*, 2547.

(11) Che, M.; Fournier, M.; Launay, J. P. *J. Chem. Phys.* **1979**, *71*, 1954.

(12) Launay, J. P.; Fournier, M.; Sanchez, C.; Livage, J.; Pope, M. T. *Inorg. Nucl. Chem. Lett.* **1980**, *16*, 257.

(13) Pope M. T. In *Mixed Valence Compounds*; Brown, D. B., Ed.; Reidel Publishing: Dordrecht, The Netherlands, 1980; p 365.

(14) Sanchez, C.; Livage, J.; Launay, J. P.; Fournier, M.; Jeannin, Y. *J. Am. Chem. Soc.* **1982**, *104*, 3194.

(15) Sanchez, C.; Livage, J.; Doppelt, P.; Chauveau, F.; Lefebvre, J. *J. Chem. Soc., Dalton Trans.* **1982**, 2439.

(16) Sanchez, C.; Livage, J.; Launay, J. P.; Fournier, M. *J. Am. Chem. Soc.* **1983**, *105*, 6817.

S0020-1669(96)01480-2 CCC: $14.00 © 1997 American Chemical Society

hexagonal belts of alternately point- and edge-sharing MoO_6 octahedra are each capped by an edge-shared Mo_3O_{13} unit. The belts are linked by six bridging oxo ligands located on the horizontal plane of symmetry. In principle, $[S_2Mo_{18}O_{62}]^{4-}$ might be expected to accept at least 18 electrons, formally reducing each $Mo^{VI}(d^0)$ center to $Mo^{V}(d^1)$. Such highly reduced species have yet to be achieved in Dawson anions. One- and two-electron reduction products of $[S_2Mo_{18}O_{62}]^{4-}$ have been reported, and a ($4e^-$, $3H^+$)-reduced form has been characterized structurally.[23,28] The meta-tungstate ion, $[H_2W_{12}O_{40}]^{6-}$, is reported to accept at least 24 electrons, together with charge-compensating protons.[2,3,29−32] This corresponds to reduction of the 12 W(VI) sites to W(IV), stabilized by intermetallic interactions. Apparently, a further eight electrons can be accepted into nonbonding levels.[29,33]

Previous electrochemical studies have demonstrated that a series of chemically reversible one-electron steps can be observed for reduction of α-$[S_2Mo_{18}O_{62}]^{4-}$ on the voltammetric time scale in aprotic media.[23,34−36] The first four processes **I**−**IV** are represented by eq 1:

$$[S_2Mo_{18}O_{62}]^{4-} \xrightleftharpoons{e^-} [S_2Mo_{18}O_{62}]^{5-} \xrightleftharpoons{e^-} [S_2Mo_{18}O_{62}]^{6-} \xrightleftharpoons{e^-} [S_2Mo_{18}O_{62}]^{7-} \xrightleftharpoons{e^-} [S_2Mo_{18}O_{62}]^{8-} \quad (1)$$

A fifth poorly defined reduction wave has been reported.[35] Consequently, it would appear that additional reduction is possible.

Voltammetric measurements at a glassy carbon electrode on $[S_2Mo_{18}O_{62}]^{4-}$ in 95/5 v/v $MeCN/H_2O$ containing 0.1 M $HClO_4$ led to the observation of six reduction waves.[26] The first four each involved transfer of two electrons, and the two most negative processes were proposed as four-electron steps. Variation of proton concentration suggested that two protons were taken up in each of the four two-electron steps:

$$[S_2Mo_{18}O_{62}]^{4-} \xrightleftharpoons{2e^-,\ 2H^+} [H_2S_2Mo^{V}{}_2Mo^{VI}{}_{16}O_{62}]^{4-} \xrightleftharpoons{2e^-,\ 2H^+} [H_4S_2Mo^{V}{}_4Mo^{VI}{}_{14}O_{62}]^{4-} \xrightleftharpoons{2e^-,\ 2H^+} [H_6S_2Mo^{V}{}_6Mo^{VI}{}_{12}O_{62}]^{4-} \xrightleftharpoons{2e^-,\ 2H^+} [H_8S_2Mo^{V}{}_8Mo^{VI}{}_{10}O_{62}]^{4-} \quad (2)$$

The possibility of isomerization was not considered. The first three reductions have been observed as reversible two-electron polarographic waves in aqueous sulfuric acid.[25] While the possibility of protonation accompanying the reduction steps was not considered explicitly, the four-electron reduced species was proposed to isomerize to the β-isomer, as observed for the equivalent compounds containing P(V) and As(V).[37] An α (D_{3h}) → β (D_{3d}) isomerization involves rotation of one of the Mo_3 caps of structure **I** by 60° around the C_3 axis.

In the present paper, we have extended the voltammetric studies on $[S_2Mo_{18}O_{62}]^{4-}$ in the aprotic medium MeCN to the very negative potential region and observe a total of eight one-electron reduction processes occurring as four adjacent pairs. In addition, in the acidic medium 95/5 v/v $MeCN/H_2O$ containing 0.02 M $HClO_4$, evidence is presented for an overall reversible reduction by at least 18 electrons, corresponding to formal reduction of the 18 Mo^{VI} centers to Mo^{V}. The work complements our previous studies of the redox chemistry of $[S_2Mo_{18}O_{62}]^{4-}$, including photochemical properties, voltammetry in micro-crystalline form, and characterization of the one-electron reduced species, $[S_2Mo_{18}O_{62}]^{5-}$.[23,36,38]

Experimental Section

Reagents. Sodium molybdate (BDH, AR grade), perchloric acid (70%, BDH, Aristar grade), Bu_4NClO_4, and Hex_4NClO_4 (Southwestern Analytical, electrometic grade), and sulfuric acid (May and Baker, AR grade) were used as received. Acetonitrile (Mallinckrodt, Chrom AR HPLC grade) was purified and stored under dry dinitrogen.[39]

α-$(Hex_4N)_4[S_2Mo_{18}O_{62}]$. H_2SO_4 (18 M; 0.27 mol; 15 mL) and MeCN (300 mL) were added consecutively to a stirred solution of $Na_2MoO_4 \cdot 2H_2O$ (0.08 mol; 18.7 g) in H_2O (60 mL). The two-phase mixture was stirred while being heated to boiling over 1 h. The upper layer turned orange. After the mixture was cooled to room temperature, the colorless lower layer was discarded. Addition of Hex_4NBr or Hex_4NClO_4 (0.035 mol) caused the formation of a yellow solid phase and an orange oily phase in contact with the major liquid phase. When precipitation of the orange oily phase was nearly complete (3−5 min), the major liquid phase was decanted and discarded. MeCN (300 mL) and H_2O (15 mL) were added to the orange oily phase. The resulting orange solution was decanted away from a small amount of yellow solid phase and stored at 4 °C for 1 day. Orange crystals were filtered, washed with EtOH and H_2O, and dried under vacuum. The product was redissolved in MeCN (80 mL) and H_2O (2 mL) and the solution allowed to stand at 4 °C for 5 days before isolation of the final orange crystalline product (7.0 g; 42%). Anal. (Analytische Laboratorien, Gummersbach, Germany) Found: C, 27.34; H, 4.87; N, 1.33; S, 1.63. $C_{96}H_{208}Mo_{18}N_4O_{62}S_2$ requires: C, 27.44; H, 5.00; N, 1.33; S, 1.53. An electrospray ionization mass spectrum (0.2 mM in MeCN; negative ion) revealed a single ion only at m/z 696 = 4202/4, corresponding to the parent ion $[S_2Mo_{18}O_{62}]^{4-}$.

Electrochemistry. All voltammograms were acquired using a Cypress Systems Model CS-1090 computer-controlled electroanalytical system in the cyclic staircase mode (with a 2 mV potential step). The standard three-electrode arrangement was employed with a Pt wire auxiliary electrode. When data were recorded in dry acetonitrile at −30 °C, a platinum wire quasi-reference electrode was employed. For all other measurements, aqueous AgCl/Ag (3 M NaCl) or Ag^+/Ag (0.01 M $AgNO_3$ in acetonitrile) reference electrodes were used. The reversible Fc^+/Fc voltammetry of 0.5 mM ferrocene was used as an external reference couple. All potentials are quoted relative to this couple (0.400 V versus standard hydrogen electrode) with an error of ±0.01 V. The working electrode for cyclic voltammetry was either a Cypress Instrument 1.0 mm diameter glassy carbon or a Bioanalytical Systems 1.8 mm diameter platinum disk.

---

(17) Harmalker, S. P.; Leparulo, M. A.; Pope, M. T. *J. Am. Chem. Soc.* **1983**, *105*, 4286.
(18) Kozik, M.; Hammer, C. F.; Baker, L. C. W. *J. Am. Chem. Soc.* **1986**, *108*, 2748.
(19) Kozik, M.; Hammer, C. F.; Baker, L. C. W. *J. Am. Chem. Soc.* **1986**, *108*, 7627 and references therein.
(20) Piepgrass, K.; Barrows, J. N.; Pope, M. T. *J. Chem. Soc., Chem. Commun.* **1989**, 10.
(21) Casan-Pastor, N.; Baker, L. C. W. *J. Am. Chem. Soc.* **1992**, *114*, 10384.
(22) Barrows, J. N.; Pope, M. T. *Inorg. Chim. Acta* **1993**, *213*, 91.
(23) Cooper, J. B.; Way, D. M.; Bond, A. M.; Wedd, A. G. *Inorg. Chem.* **1993**, *32*, 2416.
(24) Hori, T.; Himeno, S. *Chem. Lett.* **1987**, 53.
(25) Cartié, B. *J. Chem. Res. Synop.* **1988**, 290.
(26) Himeno, S.; Hori, T.; Saito, A. *Bull. Chem. Soc. Jpn.* **1989**, *62*, 2184.
(27) Hori, T.; Tamada, O.; Himeno, S. *J. Chem. Soc., Dalton Trans.* **1989**, 1491.
(28) Neier, R.; Trojanowski, C.; Mattes, R. *J. Chem. Soc., Dalton Trans.* **1995**, 2521.
(29) Launay, J. P. *J. Inorg. Nucl. Chem.* **1976**, *38*, 807.
(30) Kazansky, L. P.; Launay, J. P. *Chem. Phys. Lett.* **1977**, *51*, 242.
(31) Jeannin, Y.; Launay, J. P.; Seid Sedjadi, M. A. *Inorg. Chem.* **1980**, *19*, 2933.
(32) Piepgrass, K.; Pope, M. T. *J. Am. Chem. Soc.* **1987**, *109*, 1586.
(33) Piepgrass, K.; Pope, M. T. *J. Am. Chem. Soc.* **1989**, *111*, 753.
(34) Cooper, J. B.; Bond, A. M.; Oldham, K. B. *J. Electroanal. Chem.* **1992**, *331*, 877.
(35) Himeno, S.; Osakai, T.; Saito, A.; Maeda, K.; Hori, T. *J. Electroanal. Chem.* **1992**, *337*, 371.
(36) Bond, A. M.; Way, D. M.; Wedd, A. G.; Compton, R. G.; Booth, J.; Eklund, J. C. *Inorg. Chem.* **1995**, *34*, 3378.
(37) Souchay, P.; Contant, R.; Fruchart, J. M. *C. R. Acad. Sci.* **1967**, *264*, 976)
(38) Bond, A. M.; Cooper, J. B.; Marken, F.; Way, D. M. *J. Electroanal. Chem.* **1995**, *396*, 407.
(39) Kiesele, H. *Anal. Chem.* **1980**, *52*, 2230.

Rotating disk voltammetric measurement was undertaken with a Metrohm 2.8 mm diameter glassy carbon working electrode which was rotated by a variable speed Metrohm 628l10 rotator. Steady-state microdisk electrode voltammograms are reported at the 50 μm diameter working electrode since fouling of microdisk electrodes of smaller diameter occurred when the potential was scanned beyond either the first or second waves.

Before each voltammetric experiment, glassy carbon electrodes were polished on LECO polishing pads with 0.25 μm Buehler Ltd. Metadi diamond polishing compound, and finally with 0.05 μm polishing alumina. The condition of the platinum working electrode surfaces was maintained by frequent polishing with the 0.05 μm polishing alumina.

The 95/5 MeCN/H_2O solutions were purged with MeCN-saturated dinitrogen before the voltammetric measurements and then maintained under an atmosphere of dry dinitrogen during the course of the experiments. For experiments in MeCN, the solid polyanion salt and supporting electrolyte were placed in the electrochemical cell which was attached to a vacuum line. The system was degassed initially by heating the solids with a hot air blower. The solvent was added anaerobically and the system exposed to a series of freeze/pump/thaw cycles. Eight cycles normally led to the extension of the solvent limits available in cyclic voltammograms recorded in MeCN by approximately 1 V. The volume change occurring during this procedure was found to be negligible when using solvent volumes of 2.0−3.0 mL. For the low-temperature work, a thermocouple was included in the electrochemical cell which was immersed in an ethanol/dry ice bath maintained at −30 ± 3 °C.

Results

Synthesis. The original synthesis of $(Bu_4N)_4[S_2Mo_{18}O_{62}]$ involved recrystallization from MeCN.[24,26] The procedure provides crystalline material which becomes a powder upon exposure to vacuum, due to loss of MeCN of crystallization. Use of Hex_4N^+ as cation and recrystallization from MeCN/H_2O provides analytically pure $(Hex_4N)_4[S_2Mo_{18}O_{62}]$, which remains crystalline upon exposure to vacuum, is soluble in MeCN (>0.2 M versus 0.013 M for the Bu_4N^+ salt), and exhibits consistently clean electrochemistry.

Voltammetry in MeCN. Figure 1 shows the reduction of α-$[S_2Mo_{18}O_{62}]^{4-}$ under conditions of cyclic voltammetry at a glassy carbon electrode in dry MeCN over the potential range of +1.0 to −3.0 V versus Fc^+/Fc at scan rates of 0.05, 0.5, and 10 V s^{-1}. Clearly, an extensive and complex reductive chemistry beyond that reported to date is available.

Cyclic Voltammetry. For convenience, the previously reported processes summarized in eq 1 are designated **I**, **II**, **III**, and **IV**. Experiments as a function of scan rate at glassy carbon electrodes involved switching the potential between the various processes. A full data set is provided in Table S1 and a summary in Table 1.

Scanning the potential regions of processes **I** and **II** produced almost ideal, reversible, one-electron reduction responses for scan rates in the range 0.02 to 10 V s^{-1} (Figure 1 and supplementary text, Figure S1, and Table S1 of the Supporting Information).

However, when the potential is switched after processes **III** or **IV**, deviations from ideality emerge in the form of a dependence of $E_{1/2}$ on v and the appearance of minor processes (Figures 2 and S2; Table S1). In particular, a new chemically reversible process is present at potentials just after process **IV**, and new processes are evident between **II** and **III**. However, at a fast scan rate of 10 V s^{-1}, four almost ideal, reversible, one-electron reduction processes are observed (Figure 2c). Deliberate addition of water amplifies the relative magnitude of the minor processes, implying that the three- and four-electron reduced anions $[S_2Mo_{18}O_{62}]^{7-,8-}$, the presumed products of processes **III** and **IV**, are basic and readily protonated by adventitious water present in acetonitrile.

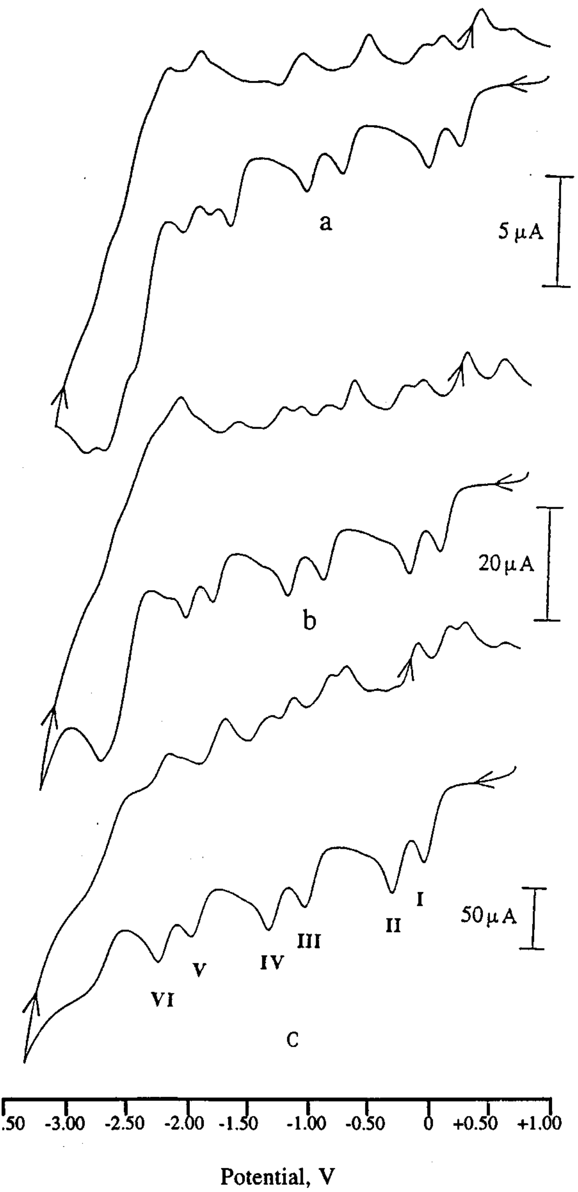

Figure 1. Cyclic voltammograms of α-$[S_2Mo_{18}O_{62}]^{4-}$ (2.0 mM) in MeCN (0.2 M Bu_4NClO_4) at a glassy carbon disk electrode (*d*, 1.0 mm) at 22 °C. Potentials versus Fc^+/Fc. Scan rate (V s^{-1}): (a) 0.05; (b) 0.50; (c) 10.

Table 1. Cyclic Voltammetric Data for α-$[S_2Mo_{18}O_{62}]^{4-}$ in MeCN[a,b]

process	*T*, °C	E_{pc}, V	$E_{1/2}$, V	$\Delta E_{1/2}$, V
I	22	+0.03	+0.10	−0.24
II		−0.21	−0.14	−0.66
III		−0.87	−0.80	−0.27
IV		−1.14	−1.07	−0.60
V		−1.74	−1.67	−0.25
VI		−1.99	−1.92	−0.55[c]
VII	−30[d]	−2.44	−2.36	−0.28
VIII		−2.72	−2.64	

[a] 2.0 mM; 0.2 M Bu_4NClO_4; *v*, 10 V s^{-1}; working electrode, glassy carbon disk (*d*, 1.0 mm). [b] Complete data given in Table S1. [c] Value observed at −30 °C. [d] A platinum quasi-reference electrode was used in these measurements. The half-wave potentials are referenced against couple **I** which was assigned a value +0.100 V. Anodic shifts of 0 to 0.1 V are observed upon change of temperature from 22 to −30 °C.

Complexity increases as more highly reduced species are generated. The effect of scan rate variation on process **V** is illustrated in Figure 3. At slow scan rates, **V** has a peak current considerably larger than that expected for a one-electron reduction process (Figure 3a). As the scan rate increases, the

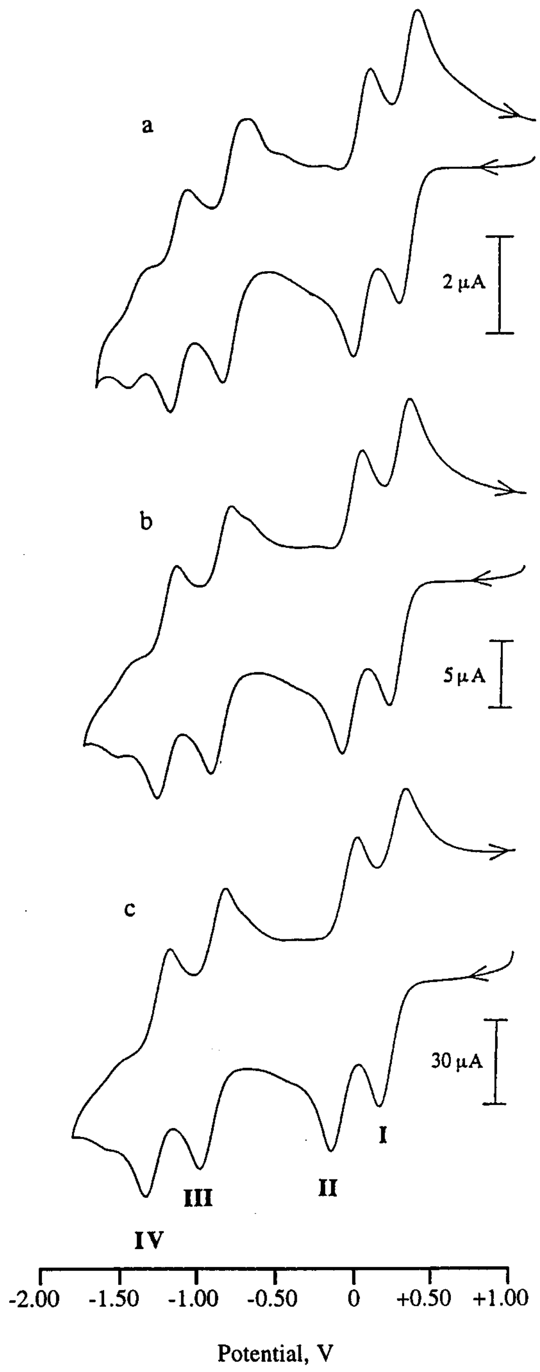

Figure 2. Effect of switching the potential after process **IV**. The conditions of Figure 1 apply. Scan rate (V s^{-1}): (a) 0.05; (b) 0.50; (c) 10.

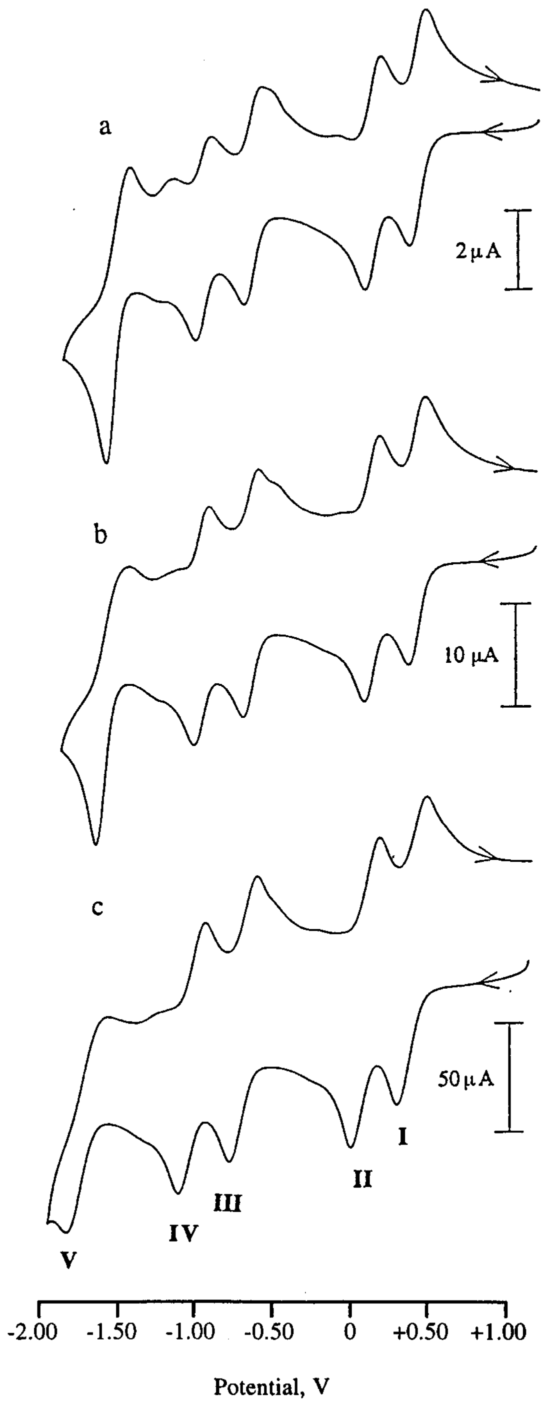

Figure 3. Effect of switching the potential after process **V**. The conditions of Figure 1 apply. Scan rate (V s^{-1}): (a) 0.05; (b) 0.50; (c) 10.

peak height of **V** approaches those of processes **I**−**IV**, its apparent E_{pc} shifts cathodically, and the anodic peak becomes broad, appearing to correspond to at least two unresolved processes (Figure 3b,c). These features are consistent with protonation of the product of process **IV**, $[S_2Mo_{18}O_{62}]^{8-}$, causing the subsequent two one-electron waves, **V** and **VI**, to shift anodically and to coalesce into a single two-electron reduction wave. At fast scan rates, insufficient time is available for full protonation to take place.

Even more complex voltammograms are seen upon switching the potential after **VI** (Figure S3). Like **V**, **VI** only converts to a one-electron process at fast scan rates when the influence of following chemical reactions is minimized. Very dry acetonitrile is required to achieve this.

Data presented so far imply that, at fast scan rates and in the absence of adventitious proton sources, processes **V** and **VI** correspond to the following simple couples, extensions of the electron transfer series of eq 1:

$$\text{V:}\quad \alpha\text{-}[S_2Mo_{18}O_{62}]^{8-} + e^- \rightleftharpoons \alpha\text{-}[S_2Mo_{18}O_{62}]^{9-} \qquad (4)$$

$$\text{VI:}\quad \alpha\text{-}[S_2Mo_{18}O_{62}]^{9-} + e^- \rightleftharpoons \alpha\text{-}[S_2Mo_{18}O_{62}]^{10-} \qquad (5)$$

Half-wave potentials $E_{1/2}$ for **I** and **II** differ by −0.24 V, and similar differences are seen for the pairs **III**, **IV** and **V**, **VI**. On the basis of a separation of about −0.6 V between individual pairs (Table 1), the first process for the next reversible pair is predicted to occur at about −2.50 V. However, switching the potential just prior to the solvent limit of −3.0 V shows complex behavior (Figure 1). At −30 °C, on the other hand, direct evidence is found for the predicted seventh and eighth processes,

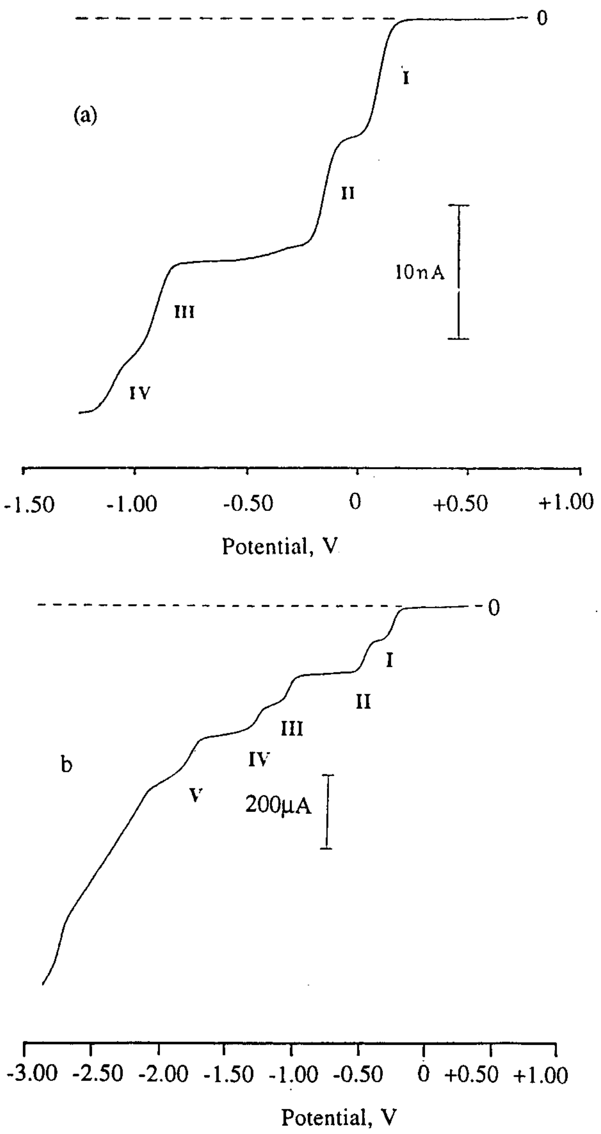

Figure 4. Steady-state voltammograms of α-$[S_2Mo_{18}O_{62}]^{4-}$ (2.0 mM) in MeCN (0.1 M Bu_4NClO_4) at 20 °C. Scan rate, 0.005 V s^{-1}. (a) Platinum microdisk electrode (*d*, 50 μm); (b) glassy carbon rotating disk electrode (*d*, 2.8 mm); rotation speed, 500 rpm.

Table 2. Near Steady-State Voltammetric Data at a Platinum Microdisk Electrode for α-$[S_2Mo_{18}O_{62}]^{4-}$ in MeCN[a]

process	$E_{1/2}$, V	($E_{1/4} - E_{3/4}$, V	i_L, nA
I	+0.10	0.055	11.9
II	−0.14	0.055	10.9
	−0.35		0.9
	−0.46		0.7
III	−0.91	0.065	9.6
IV	−1.09	0.060	5.4

[a] *d*, 50 μm; 2.0 mM; 0.1 M Bu_4NClO_4; *v*, 0.005 V s^{-1}; *T*, 20 °C.

VII and **VIII** (Figure S4; Table 1). While these processes are not completely reversible in the chemical sense, the estimated reduction potentials will not be significantly affected by the following chemical reactions. The latter are relatively slow on the voltammetric time scale.

Steady-State Voltammetry. Figure 4a shows a near steady-state voltammogram obtained at a platinum microdisk electrode (*d*, 100 μm) over the potential range encompassing waves **I**−**IV**. Parameters $E_{1/2}$, ($E_{1/4} - E_{3/4}$), and i_L are listed in Table 2. While $E_{1/2}$ values obtained for processes **I** and **II** are the same as those found in cyclic voltammetry (Table 1), technique-dependent variations in $E_{1/2}$ are evident for processes **III** and **IV**. In addition, the magnitude of the limiting currents i_L decrease steadily in the order **I** > **II** > **III** > **IV** (Table 2), implying that they are not, in fact, all simple reversible processes under these near steady-state conditions. In addition, minor processes are seen between **II** and **III** (Table 2) and account for the majority of the "missing" current for processes **II** and **III**.

For electrochemically reversible processes, plots of *E* versus $RT \ln[(i_L - i)/i]/F$ over the potential range between the quartile ($E_{1/4}$) and the three-quartile ($E_{3/4}$) potential values will be linear with intercept $E_{1/2}$ and slope $1/n$.[40a] **I** and **II** meet these requirements with $n = 1$, but **III** and **IV** do not (apparent *n* values, 0.83 and 0.87). In addition, the limiting current of **IV** is considerably smaller than that expected (Table 2). Complete electrode blockage takes place at the platinum working electrode surface soon after scanning the potential past process **IV**. The onset of this adsorption process is a plausible explanation of the much smaller limiting current value for the fourth wave.

A second series of steady-state voltammograms was recorded using a glassy carbon rotating disk electrode (*d*, 2.8 mm). Parameters are reported as a function of the rotation speed in Table S2. The voltammogram in Figure 4b shows that, in addition to **I**−**IV**, process **V** at −1.66 V is now well defined under these conditions. Scanning beyond **V** enables further processes to be observed which are attributable to multielectron reduction (at least seven electrons) of the mixture of protonated and nonprotonated species now present at the working electrode surface.

The first four processes exhibit $E_{1/2}$ values which are essentially independent of the rotation speed (Table S2). Plots of *E* versus $RT \ln[(i_L - i)/i]/F$ for each of the first three processes at a rotation speed of 500 rpm provide estimates of *n* of 0.99, 1.01, and 1.02, respectively. That for the fourth process is 0.91, suggesting a minor departure from ideality.[41] The ideal behaviors of **I** and **II** allow their total limiting current to be used to calculate the diffusion coefficient *D* of α-$[S_2Mo_{18}O_{62}]^{4-}$ in CH_3CN using the Levich equation.[40b] The value of 6.4×10^{-6} cm² s^{-1} at 20 °C can be compared with values of 6.2×10^{-6} cm² s^{-1} estimated from the microelectrode voltammetry (Table 2: $i_L = 2nFCdD$) and 5.0×10^{-6} cm² s^{-1} obtained previously at a platinum rotating disk electrode at 25 °C.[36]

Voltammetry in 95/5 MeCN/H_2O (0.02 M $HClO_4$). α-$[S_2Mo_{18}O_{62}]^{4-}$ in dry MeCN exhibits four pairs of reversible one-electron reduction waves (cf. Figure S4). Protonation of highly reduced complexes by adventitious water appears to be a cause of complications seen at more negative potentials (Figures 1 and 4b). Experiments in the presence of acid were undertaken to provide more information. In addition, the positive shifts in potential predicted by the Nernst equation upon increase in proton concentration suggested possible access to reduction processes that lie beyond the solvent limit in dry MeCN.

Cyclic Voltammetry. Voltammograms at a glassy-carbon working electrode (*d*, 1.0 mm) revealed the presence of at least seven chemically reversible reduction waves in the range 0.3 to −1.0 V (Figure 5). The processes observed in this medium are labeled I, II, etc., to distinguish them from the one-electron waves observed in MeCN which are labeled **I**, **II**, etc. Processes I−IV are well defined in the presence of 0.02 M $HClO_4$ (Figure S5). A full data set is provided in Table S3 with a summary given in Table 3.

---

(40) Bard, A. J; Faulkner, L. R. *Electrochemical Methods, Fundamentals and Applications*; Wiley: New York, 1980; (a) pp 160, 290; (b) p 288; (c) p 229.

(41) Estimates of $E_{1/2}$ from the intercepts for the four plots were +0.10, −0.13, −0.79, and −1.08 V, respectively (compare with Table 2). The correlation coefficient for the fit of the straight line plots were 1.000, 0.998, 0.973, and 0.977, respectively.

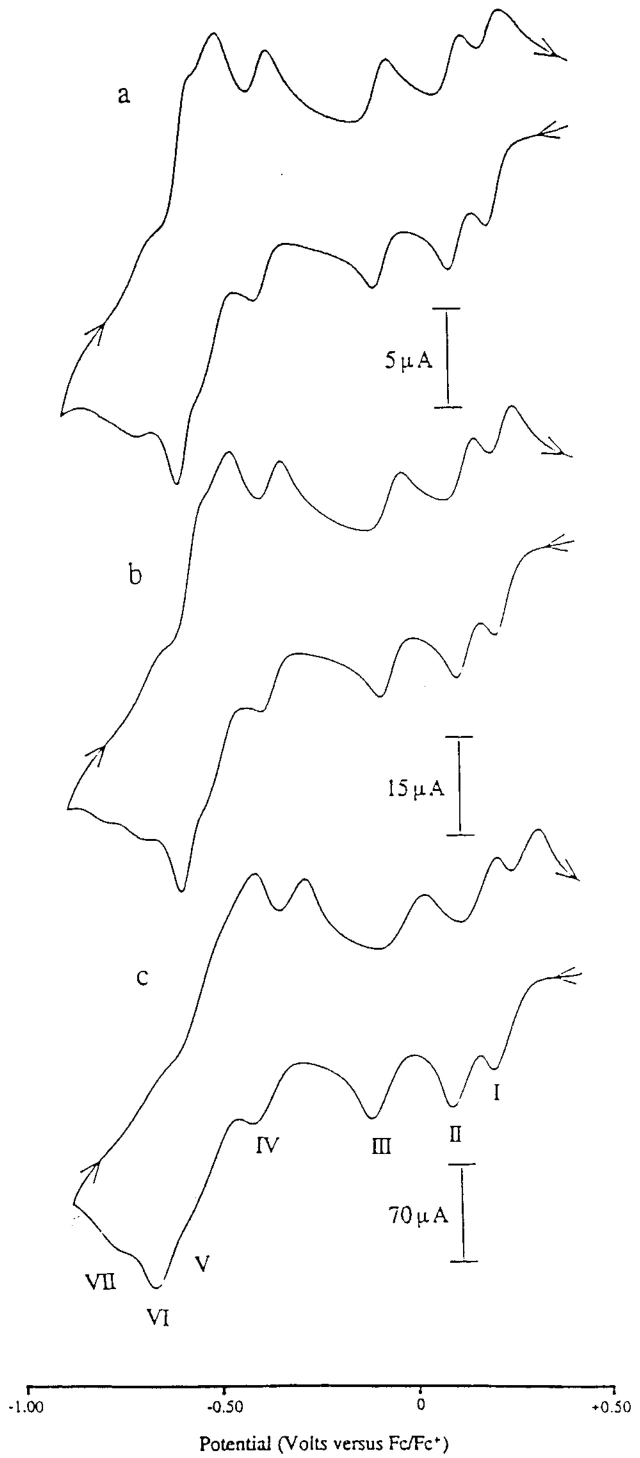

Figure 5. Cyclic voltammograms of α-$[S_2Mo_{18}O_{62}]^{4-}$ (1.0 mM) in 95/5 MeCN/H_2O (0.1 M Bu_4NClO_4; 0.02 M $HClO_4$) at a glassy carbon disk electrode (*d*, 1.0 mm) at 20 °C. Scan rate (V s^{-1}): (a) 0.05; (b) 0.50; (c) 10.

Table 3. Cyclic Voltammetric Data for α-$[S_2Mo_{18}O_{62}]^{4-}$ in 95/5 MeCN/H_2O (0.02 M $HClO_4$)

process	E_{pc}, V	$E_{1/2}$, V	$\Delta E_{1/2}$, V
I	+0.14	+0.19	−0.11
II	+0.03	+0.08	−0.20
III	−0.18	−0.12	−0.31
IV	−0.48	−0.43	

[a] 2.0 mM; 0.1 M Bu_4NClO_4; v, 10 V s^{-1}; T, 22 °C; working electrode, glassy carbon disk (*d*, 1.0 mm). [b] Complete data set given in Table S3.

Switching the potential after the first process I gave $i_{pa}/i_{pc} = 1$, as required for a chemically reversible process, and $\Delta E_p = 0.038$ V (v, 0.05 V s^{-1}), consistent with an essentially diffusion-controlled two-electron process.[40c] In addition, i_{pc} was significantly larger than that observed for the one-electron couple Fc^+/Fc under the same conditions. Our data obtained in dry MeCN, coupled with that of Himeno in acid media,[7] suggest that process I consists of two unresolved one-electron steps (processes **I** and **II**) accompanied by proton transfer reactions, rather than the simultaneous transfer of two electrons. $E_{1/2}$ for process I is 0.19 V and is independent of scan rate over the range 0.05−10 V s^{-1}. This value is more positive than those of 0.10 and −0.14 V for processes **I** and **II** (Table 1), highlighting the shift that has occurred due to the influence of additional protonation reactions which follow the electron transfer steps. Similar conclusions can be drawn about processes II−IV although $E_{1/2}$ values now depend somewhat upon v, varying by 0.02 V in the range 0.05−10 V s^{-1} (Table S3).

Processes V, VI, and VII (Figure 5) overlap, but systematic examination (see supplementary text of the Supporting Information) indicates that they are derived from groups of reversible one-electron transfer steps coupled to proton transfer reactions. The potentials of these one-electron processes are more negative than the acetonitrile solvent limit and are unobservable in that solvent (Table 1).

Switching at potentials more negative than the seventh wave reveals a further group of reduction processes between −1.0 and −1.8 V versus Fc^+/Fc (Figure S6). Examination of this group suggests that at least a further four electrons are associated with these processes.

Steady-State Voltammetry. Figure 6a shows a near steady-state voltammogram obtained at a platinum microdisk electrode (*d*, 50 µm) over the potential range encompassing waves I−IV. Again, adsorption of reduced species blocked the electrode at more negative potentials. Microdisk electrodes less than 50 µm in diameter were affected by adsorption at all potentials and could not be used. Parameters $E_{1/2}$, ($E_{1/4} - E_{3/4}$), and i_L are listed in Table 4. ($E_{1/4} - E_{3/4}$) will be 0.028 V for a reversible process with simultaneous transfer of two electrons.[40a] The observed values for processes III and IV are larger, implying that they do not involve simultaneous transfer of two electrons at the same potential.

Plots of E versus $RT \ln[(i_L - i)/i]/F$ for waves I and II provide n values of 2.1 and 1.9 (±0.1), as expected for simple reversible two-electron charge transfer processes. The intercepts provide $E_{1/2}$ values (Table 4) similar to those found in cyclic voltammetry (Table 3). Waves III and IV gave apparent n values of 1.6 and 1.5 electrons, respectively, based on the assumption that they are simple reversible processes. Clearly, they are not. However, essentially equivalent limiting currents for each of the four waves confirm that all four processes involve the overall transfer of two electrons (Table 4). While processes III and IV are chemically reversible, it is apparent again that they do not originate from simple two-electron charge transfer events.

Figure 6b shows a steady-state voltammogram at a glassy carbon rotating disk electrode (*d*, 2.8 mm) at a rotation speed of 500 rpm. Well-defined processes are seen out to −1.5 V. Limiting currents as a function of rotation rate are presented in Table S4 while results for processes I−IV obtained at a rotation speed of 500 rpm are summarized in Table 4. Similar conclusions to those drawn from the above microelectrode work can be made about processes I−IV.

A current of 21 ± 1 µA is associated with the transfer of one electron at a rotation rate of 500 rpm (Table 4). The total current associated with processes V−VII (Figure 6b) is 210 ± 4 µA, equivalent to the transfer of 10 electrons. This conclusion is sustained for rotation rates in the range 500−3000 rpm (Table S4). The combined cyclic and steady-state voltammetry data

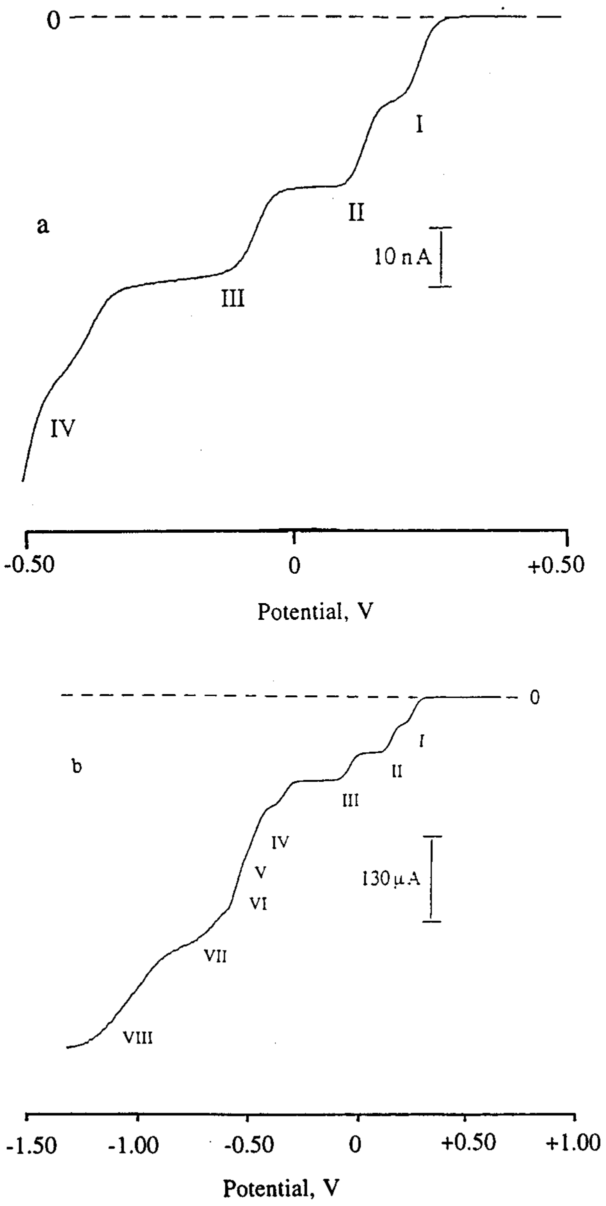

Figure 6. Steady-state voltammograms of α-$[S_2Mo_{18}O_{62}]^{4-}$ (2.0 mM) in 95/5 MeCN/H_2O (0.1 M Bu_4NClO_4; 0.02 M $HClO_4$) at 20 °C. Scan rate, 0.005 V s^{-1}. (a) Platinum microdisk electrode (*d*, 50 μm); (b) glassy carbon rotating disk electrode (*d*, 2.8 mm); rotation speed, 500 rpm.

indicate that waves V, VI, and VII involve a total of 10 electrons in the ratios 4:4:2. A total of 18 electrons has been added to the $[S_2Mo_{18}O_{62}]^{4-}$ anion at this point to produce a (protonated) product, which is stable on the short time scale of these voltammetric experiments. The limiting current of wave VIII indicates that at least eight further electrons can be transferred in a subsequent series of unresolved processes.

An equivalent series of measurements were carried out in the presence of 0.20 M $HClO_4$, i.e., at an acid concentration increased by a factor of 10. Processes I−VIII were again observable. They were shifted anodically by the increased proton concentration, but the separation between processes remained similar. However, processes V−VII were better resolved (Figure S7), confirming the ratios of limiting currents as 4:4:2.

Discussion

The total data indicate that eight reversible one-electron reductions of $[S_2Mo_{18}O_{62}]^{4-}$, occurring as four adjacent pairs, are accessible in MeCN (cf. Figure S4). The difference in potential within each pair is remarkably constant, 0.26 ± 0.02 V, as are the separations between adjacent pairs, 0.60 ± 0.06 V (Table 1). The one-electron reduction product of process **I**, $[S_2Mo_{18}O_{62}]^{5-}$, is stable to disproportionation:[23]

$$2[S_2Mo_{18}O_{62}]^{5-} \rightleftharpoons [S_2Mo_{18}O_{62}]^{4-} + [S_2Mo_{18}O_{62}]^{6-} \qquad K = 8.8 \times 10^{-5} \quad (5)$$

The same is true of the other odd electron species $[S_2Mo_{18}O_{62}]^{7-,9-,11-}$ produced by processes **III**, **V**, and **VII** (Table 1; Figure S4). The one-electron reduced anion $[P_2Mo_{18}O_{62}]^{7-}$ is also stable to disproportionation under aprotic conditions.[22]

The influence of chemical reactions which follow electron transfer increases markedly with the number of electrons n added. The effect upon the voltammetry is minimal for $n = 1-4$ (processes **I**−**IV** of Figures 2 and 4) but dominates after that, except at the shortest time scales (Figures 1, 3, 4b, and S3). The dominant following reaction in the present system is rapid protonation of highly reduced species by trace water. Protonation of $[S_2Mo_{18}O_{62}]^{8-}$ ($n = 4$), the product of process **IV**, is thermodynamically favorable, inducing anodic shifts in reduction potentials. This effect rationalizes the anodic shifts and two-electron behavior observed for process **V** at low scan rates (Figure 3).

Disproportionation of $[S_2Mo_{18}O_{62}]^{5-}$, the product of **I**, is induced by acid (cf. eq 6):[23]

$$2[S_2Mo_{18}O_{62}]^{5-} + 2H^+ \rightarrow [S_2Mo_{18}O_{62}]^{4-} + [H_2S_2Mo_{18}O_{62}]^{4-} \quad (6)$$

Equivalent acid-induced disproportionation of $[S_2Mo_{18}O_{62}]^{7-,9-}$, the products of processes **III** and **V**, are further sources of the complex behavior seen in Figures 2 and 3. Redox-induced isomerization is another possible complication.[25] Previous studies have shown that the one-electron reduced forms of α,β-$[X_2Mo_{18}O_{62}]^{6-}$ (X = P, As) are unstable to disproportionation in the presence of protons.[5,22,42,44]

The product of process **V** in MeCN, $[S_2Mo_{18}O_{62}]^{9-}$ (n = 5), has a significant lifetime on the voltammetric time scale (Figures 3c, 4b). However, more highly reduced species will all be protonated. Although a total of 12 electrons can be added to $[S_2Mo_{18}O_{62}]^{4-}$ in MeCN (Figure 6b), $[S_2Mo_{18}O_{62}]^{16-}$ is not formed in the present experiments. Some or all of the chemical reactions which follow reduction are contributing to the numerous extra processes observed in the reverse scans after switching the potential at negative values (Figures 1−3, S4, S5).

This interpretation is supported by the behavior seen in the presence of added acid. Reduction of α-$[S_2Mo_{18}O_{62}]^{4-}$ in 95/5 MeCN/H_2O (0.02 M $HClO_4$) exhibits four two-electron, chemically reversible steps. The separations in $E_{1/2}$ values are −0.11, −0.20, and −0.31 V (Table 3), i.e., every two electrons (with accompanying protons) transferred to the α-$[S_2Mo_{18}O_{62}]^{4-}$ anion causes a −0.1 V stabilization of the molecular framework with respect to further reduction. In the absence of acid, the separation between adjacent pairs of one-electron reductions is constant at about −0.6 V (Table 1). The high basicity of the unprotonated reduced species is apparent and it can be concluded that process I is derived from processes **I** and **II**, process II from **III** and **IV**, process III from **V** and **VI**, and process IV from **VII** and **VIII**.

---

(42) Contant, R.; Fruchart, J. M. *Rev. Chim. Miner.* **1974**, *11*, 123.
(43) Jeannin, Y.; Launay, J. P.; Sanchez, C.; Livage, J.; Fournier, M. *Nouv. J. Chim.* **1980**, *4*, 587.
(44) Papaconstantinou, E.; Hoffman, N. Z. *Inorg. Chem.* **1982**, *21*, 2087.

Table 4. Steady-State Voltammetric Data for α-$[S_2Mo_{18}O_{62}]^{4-}$ in 95/5 MeCN/H_2O (0.02 M $HClO_4$)[a]

	platinum microdisk electrode[b]				glassy carbon rotating disk electrode[c]			
process	$E_{1/2}$,[d] V	$(E_{1/4} - E_{3/4})$, V	i_L, nA	*n*	$E_{1/2}$,[f] V	$(E_{1/4} - E_{3/4})$ V	i_L,[f] μA	*n*[e]
I	0.19	0.028	−14.0	2[d,e]	0.19	0.034	−41.5	2
II	0.09	0.028	−15.0	2[d,e]	0.09	0.032	−42.5	2
III	−0.11	0.036	−15.0	2[e]	−0.11	0.038	−41.5	2
IV	−0.41	0.038	−13.5	2[e]	−0.40	0.040	−39.0	2

[a] 2.0 mM; 0.1 M Bu_4NClO_4; *v*, 0.005 V s^{-1}; *T*, 20 °C. [b] *d*, 50 μm. [c] *d*, 2.8 mm. [d] Estimated from plots of *E* versus $RT \ln[(i_L - i)/i]/F$. [e] Estimated from i_L values. [f] Estimated from data at 500 rpm.

The anodic Nernstian shifts in reduction potential induced by higher proton concentration allows observation of an 18-electron reduced species, the product of process VII. This species is stable on the voltammetric time scale (Figures 5, 6b, and S7) and corresponds to formal reduction of all Mo(VI) centers in α-$[S_2Mo_{18}O_{62}]^{4-}$ to Mo(V). A further eight electrons can be added (Figure 6b). This behavior is similar to that reported for $[H_2W_{12}O_{40}]^{6-}$ where a 24-electron reduction of all W(VI) centers to W(IV) occurs with the formal generation of 12 W−W bonds. A further eight electrons can be accepted into nonbonding levels.[26]

The present work can be related to the pioneering electrochemical work of Pope and Papaconstantinou on $[PW_{12}O_{40}]^{5-}$ and $[X_2M_{18}O_{62}]^{6-}$ (X = P, As; M = Mo, W) in aqueous sulfate solution.[5,6] At sufficiently high pH, six successive one-electron processes are observed for $[PW_{12}O_{40}]^{3-}$ and $[P_2W_{18}O_{62}]^{6-}$, occurring as three adjacent pairs. The difference in potential within each pair is about 0.2 V, and the separation between adjacent pairs is about 0.25−0.6 V (cf. Table 1). The two pairs at more negative potentials coalesce to two-electron processes below pH 4 (cf. Table 4), as does the third pair in concentrated acid.[45] $[P_2Mo_{18}O_{62}]^{6-}$ is more easily reduced than its tungsten analog, and its reduced anions are stronger bases.[5] Consequently, three successive two-electron processes are seen at pH <10. As for the present system, two protons appear to accompany each two-electron transfer.[26]

These systems are all characterized by adjacent pairs of one-electron reductions which coalesce to overall two-electron processes in the presence of acid. Such periodicity suggests a structural basis. The structure of $[P_2W_{18}O_{62}]^{6-}$ is close to the D_{3h} representation of structure **I**.[46] In the molybdenum analog, alternating molybdenum atoms in the two hexagonal belts are displaced so that the belts are puckered, reducing the point symmetry to D_3. This gives rise to chirality.[47] The distortion is present but much less developed in $[S_2Mo_{18}O_{62}]^{4-}$ and nearly disappears in the ($4e^-$, $3H^+$)-reduced form.[27,28] The mean deviation of the molybdenum atoms from the two least squares planes decreases from 0.18 to 0.007 Å.

On the EPR time scale, the unpaired electron in $[S_2Mo_{18}O_{62}]^{5-}$ is delocalized over the whole molecular framework, an observation which correlates with a small thermal barrier of 0.0045 eV to intramolecular electron transfer.[23] Localization of added electrons will vary with the details of each system: thermal barriers in other polyoxomolybdates vary from 0.03 to 0.3 eV.[16] For example, EPR experiments show that the unpaired electron in α-$[P_2Mo_{18}O_{62}]^{7-}$ is localized in the 12 molybdenum centers of the hexagonal belts while, on the ^{17}O and ^{31}P NMR time scales, the two added electrons in α-$[P_2Mo_{18}O_{62}]^{8-}$ are trapped on adjacent atoms, one from each belt.[22,48] The two octahedra are linked by a bridging oxo ligand, and such an arrangement is consistent with the pronounced stability of the spin-paired $[Mo^VO]_2(\mu\text{-}O)$ fragment in Mo(V) chemistry.[49] On the other hand, the ^{183}W NMR spectrum of α-$[P_2W_{18}O_{62}]^{8-}$ shows that the two added electrons are spin-paired and delocalized over the 12 belt centers, on different but not necessarily adjacent sites.[18,21]

The observation of closely spaced pairs of one-electron reductions (separated by about 0.2 V) suggests a significant contribution of $M^V{}_2$ pairs to the total superexchange stabilization. The separation of 0.6 V between adjacent redox pairs in the $[S_2Mo_{18}O_{62}]^{4-}$ system is a measure of Coulombic repulsion disfavoring further reduction. In MeCN, four pairs of one-electron reductions can be detected for $[S_2Mo_{18}O_{62}]^{4-}$ before the extreme basicity of the reduced anions leads to protonated species via scavanging of trace water. In the presence of acid, the stabilization ensuing from proton-induced disproportionation of odd electron species converts the four one-electron pairs into four overall two-electron reductions. The addition of a further 10 electrons occurs over a potential interval of 0.3 V only (processes V−VII of Figure 6b). This signals a major change in electronic structure or the level of protonation in the 18-electron reduced species.

The one-electron reduction processes (cf. Figure 4) seen at lower H^+ concentrations convert to two-electron processes at higher H^+ concentrations (cf. Figure 6). Simulation of the experimental voltammograms at intermediate H^+ concentrations provides estimates of $E_{1/2}$ values, protonation constants, and disproportionation constants for the various reduced forms of $[S_2Mo_{18}O_{62}]^{4-}$.[50] Access to such detailed information has permitted directed synthesis of the following reduced forms, all isolated as crystalline salts: (1 e^-), (2 e^-), (2 e^-, 1 H^+), (2 e^-, 2 H^+), (4 e^-, 2 H^+), (4 e^-, 4 H^+).[23,50]

Acknowledgment. A.G.W. and A.M.B. thank the Australian Research Council for support via Grant A29531579.

Supporting Information Available: Supplementary text containing a description of the cyclic voltammetry of processes I and V−VII, Tables S1−S4 listing voltammetric data, and Figures (S1−S7) of voltammograms (17 pages). Ordering information is given on any current masthead page.

IC961480R

---

(45) Keita, B.; Nadjo, L. *J. Electroanal. Chem.* **1987**, *227*, 77.

(46) Dawson, B. *Acta Crystallogr.* **1953**, *6*, 113.

(47) Pope, M. T. *Inorg. Chem.* **1976**, *15*, 2008.

(48) Kazanskii, L. P.; Fedotov, M. A. *J. Chem. Soc., Chem. Commun.* **1980**, 644.

(49) Steifel, E. I. *Prog. Inorg. Chem.* **1977**, *22*, 1.

(50) Way, D. M.; Cooper, J. B.; Sadek, M.; Vu, T.; Mahon, P. J.; Bond, A. M.; Brownlee, R. T. C.; Wedd, A. G. *Inorg. Chem.*, submitted for publication.